



NIH PUBLIC ACCESS

Author Manuscript

Biomaterials. Author manuscript; available in PMC 2012 February 1.

Published in final edited form as:

Biomaterials. 2011 February ; 32(5): 1446–1453. doi:10.1016/j.biomaterials.2010.10.052.

Tissue Integration of Growth Factor-Eluting Layer-by-Layer Polyelectrolyte Multilayer Coated Implants

Mara L. Macdonald^{1,2}, Raymond E. Samuel², Nisarg J. Shah², Robert Padera⁴, Yvette M. Beben³, and Paula T. Hammond^{2,*}¹ Harvard MIT Division of Health Sciences and Technology, Cambridge, MA, USA² Department of Chemical Engineering, Massachusetts Institute of Technology, Cambridge, MA, USA³ Department of Biology, Massachusetts Institute of Technology, Cambridge, MA, USA⁴ Department of Pathology, Brigham and Women's Hospital, Boston, MA, USA

Abstract

Drug eluting coatings that can direct the host tissue response to implanted medical devices have the potential to ameliorate both the medical and financial burden of complications from implantation. However, because many drugs useful in this arena are biologic in nature, a paucity of delivery strategies for biologics, including growth factors, currently limits the control that can be exerted on the implantation environment. Layer-by-Layer (LbL) polyelectrolyte multilayer films are highly attractive as ultrathin biologic reservoirs, due to conformal coating of difficult geometries, aqueous processing likely to preserve fragile protein function, and tenability of incorporation and release profiles. Herein, we describe the first LbL films capable of microgram-scale release of the biologic Bone Morphogenetic Protein 2 (BMP-2), which is capable of directing the host tissue response to create bone from native progenitor cells. Ten micrograms of BMP-2 are released over a period of two weeks *in vitro*; less than 1% is released in the first 3 hours (compared with commercial collagen matrices which can release up to 60% of BMP-2, too quickly to induce differentiation). BMP-2 released from LbL films retains its ability to induce bone differentiation in MC3T3 E1S4 preosteoblasts, as measured by induction of alkaline phosphatase and stains for calcium (via Alizarin Red) and calcium matrix (via Von Kossa). *In vivo*, BMP-2 film coated scaffolds were compared with film coated scaffolds lacking BMP-2. BMP-2 coatings implanted intramuscularly were able to initiate host progenitor cells to differentiate into bone, which matured and expanded from four to nine weeks as measured by MicroCT and histology. Such LbL films represent new steps towards controlling and tuning host response to implanted medical devices, which may ultimately increase the success of implanted devices, provide alternative new approaches toward bone wound healing, and lay the foundation for development of a multi-therapeutic release coating.

1. Introduction

Although protein and peptide based therapeutics represent 13% of total pharma sales and a growing fraction of approved new therapies in the US [1], several problems still remain in

* Author to whom correspondence should be addressed: hammond@mit.edu.

Publisher's Disclaimer: This is a PDF file of an unedited manuscript that has been accepted for publication. As a service to our customers we are providing this early version of the manuscript. The manuscript will undergo copyediting, typesetting, and review of the resulting proof before it is published in its final citable form. Please note that during the production process errors may be discovered which could affect the content, and all legal disclaimers that apply to the journal pertain.

biologic drug delivery, including a paucity of strategies for release of bioactive molecules from implanted medical devices. The success of these life-saving devices, including orthopaedic implants and cardiovascular devices, is critically linked to host tissue response, with failure resulting in poor patient outcomes. Complications from orthopaedic hip implants alone amass \$1 billion per year in losses in the US [2]. Therefore, the ability to coat these implanted devices to direct the molecular environment of this host cell/surface interface becomes crucially important. Herein, we report the characteristics of a polyelectrolyte multilayer nanolayered thin film able to deliver sufficient doses of a therapeutic protein to direct the host cell response from virtually any surface, regardless of geometry or surface chemistry, with release that is tunable and locally sustained.

Traditional covalent surface attachment strategies and bulk polymer release systems each fail to reach the full potential of this surface modification strategy. The limited quantity involved in direct surface attachment of proteins hampers achievable dose, and loss of activity can result from the use of covalent linkages. Bulk polymer systems such as polylactic acids or polycaprolactones are not as easily coated onto complex medical device geometries in a conformal manner, and typically are prepared as blends with the polymer in harsh solvents or at high temperatures that inactivate proteins. Surface release chemistries and polymer breakdown products from more acidic polymer degradation products can yield localized low pH conditions that further damage protein drugs [3].

Layer-by-Layer (LbL) assembly, in which a charged substrate is alternately dipped in positively and negatively charged polymer baths to build a nanolayered thin film, has recently been explored as a means of release of drugs of all kinds from surfaces [4–8]. LbL is unique in its ability to sequester high concentrations of biologic drugs for controlled local delivery using room temperature, mild aqueous conditions that preserve fragile protein activity. Precise control can be exerted on the architecture of the film, allowing compartmentalization and thus sequential release [9]; the drug load can be easily tuned with the number of layers incorporated [10]. However, in the past, thin film methods in general have been unable to achieve the microgram doses of biologics necessary for directing host tissue response; in fact, for recently explored LbL systems, films have been unable to mount a sufficient dose (usually nanogram quantities) or control over release to act as independent localized therapeutic depots (e.g., without co-implantation with stem cells) [11,12].

Herein, we characterize a LbL protein drug delivery system able to achieve multi-week, microgram scale delivery of growth factors capable of directing *in vivo* host cell behavior. Our approach is to use a tetralayer architecture utilizing 1) Poly2, a synthetic, intrinsically *tunable* cationic polymer which is a poly(β -aminoester) [13,14], 2) a biological polyanion, chondroitin sulfate, and 3) a growth factor of interest. Here we use Bone Morphogenetic Protein 2 (BMP-2), a therapeutic protein known to be able to induce native progenitor cell differentiation to the bone lineage. It is highly anticipated that local BMP-2 release from hip implants will aid in tissue ingrowth onto implants, leading to more stable fixation and better surgical outcomes [15]; ideally, release of such factors in sufficient quantity can lead to recruitment of progenitor cells within the body without the need to introduce cultured stem cells upon implantation. Poly2 is a member of the family of poly (β -aminoester)s (PBAEs), which are hydrolytically degradable through the ester linkage and have been extensively studied in gene therapy, tissue engineering, and have been shown to exhibit sequential delivery applications from multilayer films with appropriate architectures [9,13]. Here, LbL was used to conformally coat the complex geometries of a 3-dimensionally printed β -tricalcium phosphate/polycaprolactone (3DP β TCP/PCL) scaffold to induce bone formation on an implanted surface that would otherwise be unable to direct such a biological response.

2. Materials and Methods

2.1 Materials

Chondroitin sulfate sodium salt (Mn = 60000) was obtained from VWR Scientific (Edison NJ). Poly (β -aminoester) 2, hereafter called Poly 2, was synthesized as previously described [14]. Recombinant human BMP-2 (rhBMP-2) was obtained from Insight Genomics (Falls Church, VA). BMP-2 ELISA kits were obtained from Peptestech (Rocky Hill, NJ). Sodium acetate buffer, 3M was obtained from Sigma Aldrich (St. Louis, MO).

2.2 Preparation of polyelectrolyte solutions

Poly 2 dipping solutions were 2 mg/mL in 25 mM sodium acetate buffer, pH 5.1. Chondroitin dipping solution consisted of 2 mg/mL chondroitin in deionized water (18.2 M3, Milli-Q Ultrapure Water System, Millipore). rhBMP-2 dipping solutions were 50 μ g/mL in 100 mM sodium acetate buffer, pH 5.1. Poly 2 and chondroitin dipping solutions were replaced and an additional 50 μ g/mL of BMP-2 was added to the pre-existing bath, every 24 hours. All wash baths were deionized water.

2.3 Film construction and characterization

Therics™ polycaprolactone/ β -tricalcium phosphate (PCL/BTCP) co-polymer blend 3D printed scaffolds were plasma etched with room air using a Harrick PDC-32G plasma cleaner on high RF power for 1 minute and immediately immersed in Poly2 solution. A nanolayered film was fabricated on this scaffold with a Carl Zeiss HMS programmable slide stainer with the following dipping protocol: 5 minutes in Poly 2 solution, 3 washes (10, 20, 30 s), 5 minutes in chondroitin solution, 3 washes (10, 20, 30 s), 10 minutes in BMP-2 solution, 1 wash (10s) and 5 minutes in chondroitin solution with 3 washes (10, 20, 30 s).

2.4 Release characterization

BMP-2 film coated scaffolds were released at 37°C into 1 mL of growth medium, consisting of α MEM supplemented with 10% fetal bovine serum and 1% penicillin streptomycin (Invitrogen, Carlsbad CA). At a series of different time points, 0.5 mL of medium and eluted material was removed and 0.5 mL of fresh release medium was replaced. Samples were analyzed using ELISA development kits according to manufacturer instructions and cell differentiation assays (see below).

2.5 Cell culture

MC3T3-E1 Subclone 4 (ATCC, Manassas, VA) were maintained in growth medium and split when subconfluent. MC3T3-E1 cells were seeded at 1×10^4 cells/cm² and allowed to grow to confluence in 96 well plates (quantification) and in 8 well chamber slides (visualization) in 100 μ L of growth medium. MC3T3-E1 cells were cultured under four experimental conditions: (1) growth medium, (2) differentiation medium (growth medium supplemented with 50 μ g/ml L-ascorbic acid and 10 mM β -glycerol phosphate), (3) differentiation medium supplemented with 90 ng/mL of BMP-2, and (4) differentiation medium supplemented with 90 ng/mL of PEM-released BMP-2. Cell culture media were changed every two days until analysis for alkaline phosphatase, alizarin red, or Von Kossa as described below.

2.6 Alkaline phosphatase activity assay

Alkaline phosphatase (ALP) activity was determined on day 6 after the initiation of MC3T3-E1 osteogenic differentiation by visual staining techniques and quantitation of the enzyme activity. Cells were rinsed with PBS without Ca²⁺ and Mg⁺ and incubated in a stain solution consisting of 50 mM Tris HCL pH 8.0 with 1 mg/mL fast red and 1% naphthol AS-MS

dissolved in DMSO for 30 minutes at 37°C. An equal volume of 8% paraformaldehyde was added for 10 minutes at room temperature to fix cells. After rinsing 2x with distilled water, cells were imaged using a Zeiss inverted microscope with a 10X objective lens and Imaging software. The stain was solublized by adding 0.1% triton in PBS and then freezing to -80°C for one freeze-thaw cycle. The cell lysates were transferred to an eppendorf tube, centrifuged at 15,000g for 3 min at 4°C, and the supernatant was collected. Fifty µL of lysate was incubated with 150 µL of pNPP solution for 30 min at 37°C. The reaction was terminated with 0.1 M NaOH and ALP activity read on a plate reader at 405nm. The ALP activity measurements were normalized to total protein determined by BCA assay.

2.7 Alizarin red S differentiation assays

After 28 days of exposure to differentiation medium, MC3T3-E1 cells were assayed for calcium deposition using Alizarin red S (ARS). Cells were washed with PBS and fixed with 4% paraformaldehyde for 10 minutes. After three rinses of 5 min in distilled water, ARS stain solution (2% ARS in distilled water pH balanced to 4.1 with 10% ammonium hydroxide) was incubated with cells for 20 min at room temperature. Cells were then washed in distilled water 4 times for 5 minutes each. The ARS stained cultures were imaged with phase contrast microscopy.

The ARS stain was quantified using a previously published protocol [16]. The ARS stained cultures were incubated in 10% acetic acid for 30 minutes at room temperature and then the cell layers were disrupted by the use a pipette tip. The cell suspensions were transferred to a microcentrifuge tube, vortexed for 30s, paraffin wrapped and heated at 85°C for 10 min. After transferring to ice for 5 min, the tubes were centrifuged at 16,000 g for 15 minutes and pH balanced with 10% ammonium hydroxide to 4.1–4.5 pH units. Duplicates were read on a 96-well plate with black sides and a clear bottom at 405 nm.

2.8 Von Kossa differentiation assay

Von Kossa staining was performed to determine the presence of mineralization nodules within the MC3T3-E1 cell cultures. Cultures were rinsed with PBS, fixed with 4% PFA for 10 minutes, and then washed in distilled water. The cultures were then incubated in a 3% aqueous silver nitrate solution for 30 minutes at 37°C. The silver nitrate stained cultures were then treated in a UV Stratalinker under UV light at 254 nm. The cultures were washed with distilled water and then neutralized with 5% sodium thiosulfate for 5 minutes at room temperature. A final wash with distilled water was performed and the cultures were imaged by phase contrast microscopy.

2.9 Intramuscular bone formation model

All animal work was performed in accordance with protocols approved by the Committee on Animal Care at the Massachusetts Institute of Technology. Sixteen 350–400 g male Sprague Dawley rats were given preoperative analgesics (1mg/kg meloxicam and 0.05 mg/kg buprenex), and intraoperative anesthesia via 1–3% isoflurane in oxygen. The right hindlimb of each animal was shaved, cleaned with alcohol and povidone iodine solutions, and sterile drapes were placed around the surgical area. A 2 cm longitudinal incision, centered at the midshaft of the femur, was made laterally along the hindlimb. A pocket made in the quadriceps muscle mass by blunt dissection anterior to the iliotibial band. One LbL-coated PCL/BTCP scaffold was inserted into the intramuscular pocket, and wounds were closed progressively with three layers of sutures (muscle, subcutaneous, and dermal layers). Each hindlimb was implanted with either a control scaffold, [P2/chondroitin sulfate]₂₀₀, or a BMP-2 scaffold, [P2/chondroitin sulfate/rhBMP-2/chondroitin sulfate]₁₀₀. Postoperatively, rats were treated with buprenex and meloxicam until signs of distress dissipated. Rats were housed in separate cages with free access to food and water. At four and eight week time

points, four rats implanted with the control scaffold and four rats implanted with the BMP-2 scaffold were sacrificed and the implants retrieved for analysis as described below.

2.10 Micro-computed tomography (MicroCT) analysis

Excised samples were immediately placed in 10% neutral buffered formalin and imaged with MicroCT (eXplore Locus, GE Medical Systems, London, Ontario) at a resolution of 27 μm with proprietary software included with the system (EVS Evolver, GE Medical Systems, Fairfield, CT). The scanning protocol was performed with a 2000 ms shutter speed, 1 \times 1 bin size, at X-ray tube parameters 80kV and 450 μA . Four hundred images were taken at incremental angles, and rendered 3D images were reconstructed with the Reconstruction Utility and analyzed using MicroView (GE Healthcare, Fairfield, CT). Threshold values were chosen by visual inspection and kept constant across 1 month or 2 month data sets. Three independent regions of interest (ROIs) were chosen per sample, and the bone analysis tool was used to measure bone mineral density and stereology measurements of each sample. Three dimensional representations of bone formation and two dimensional digital slices through the samples were also taken for qualitative comparison.

2.11 Histological analysis

After 24 hours in 10% formalin, tissues were transferred to solutions of 70% ethanol prior to decalcification. Tissues were decalcified for 5 days in a solution of 15% EDTA and 10% sodium citrate buffer, pH 7.2 at 4°C under continuous stirring. Tissues were then serially sectioned, routinely processed, and embedded in paraffin. Microscope sections (4 μm) were stained with hematoxylin and eosin (H&E), Alcian Blue, and Masson's trichrome stains.

3. Results and Discussion

BMP-2 has an isoelectric point of 8.5, a molecular weight of 32 kDa, and is a positively charged protein under the LbL dipping conditions described herein (pH 5.1). The poly(β -aminoester)s also exhibit positive charge due to the amine groups along the backbone [17]. Hence, a tetralayer architecture was required to incorporate both cationic molecules into an electrostatically driven LbL multilayer thin film. In previous work with the model protein lysozyme, which has similar molecular weight and isoelectric point to BMP-2 [6], the natural polyanion chondroitin sulfate has been shown to have excellent electrostatic binding properties, as well as desirable protein loading and release characteristics and retention of bioactivity in LbL films. We therefore used chondroitin sulfate to create tetralayers with the following architecture (Figure 1): [Poly2/chondroitin sulfate/BMP-2/chondroitin sulfate]_n, where the term in brackets represents the architecture of one tetralayer repeat unit and n denotes the number of tetralayer units deposited.

Of the family of poly(β -aminoester)s available, Poly2 (Figure 2, structure) was chosen (i) because it affords all of the positive characteristics of this class of polymers, including biocompatibility, ease of manufacture, hydrolytic degradation, and positive charge, while (ii) additionally providing a more sustained release profile compared to other polymers [6]. The prolonged half-life of Poly2 is due to the presence of a hydrophobic region near the ester bond and a consequent decrease in water attack on the bond, hence a slower degradation rate of the polymer. In previous work, we have shown that the advantageous characteristics of an increased hydrophobic region on delaying degradation were found to balance with a point in which the polymer no longer had sufficient ionic cross-links to avoid bulk release [18]; Poly2 therefore balances increased release time with enough electrostatic backbone charge to generate very stable electrostatic LbL films.

In Figure 3, the film growth of [P2/chondroitin/BMP-2/chondroitin] films deposited on planar substrates is confirmed using profilometry measurements of film thickness. This formulation exhibits a classic multilayer exponential buildup behavior ($R^2 = 0.96$), with each tetralayer incorporating more material than the last. An exponential building behavior indicates that an interdiffusive process is taking place in which polymers adsorb to the top of the film while also penetrating into the bulk of the built film [19–22]. This type of building behavior is most frequently seen in biological systems where the charge density along the polymer backbone is lower, leading to a lower ionic crosslink density and a loopier polymer architecture [6], or in the case of small molecules which have fewer electrostatic interactions to break and therefore diffuse more readily [8,23]. It is hypothesized that the dip time and the diffusivity of the polymer lead to one region at the top of the film under constant rearrangement with each dip bath; underneath is a reorganized region that is inaccessible to polymer diffusion due to the short periods of dipping. At 2–3 microns for a 100 tetralayer film, the LbL films discussed in this paper are much thicker than the typical LbL multilayer film. These LbL films therefore have the unique advantage of an effective reservoir large enough to allow significant drug encapsulation. However, this LbL coating remains orders of magnitude thinner than traditional bulk degradation polymer delivery models [24,25] (that are typically millimeter to sub-millimeter in scale) and is conformal to the coated surface, allowing applicability to a wide variety of existing implant technologies.

A three dimensional, porous scaffold was used for in vitro and in vivo testing as a model implant. A macroporous scaffold made of osteoconductive, biocompatible elements was chosen for the following three reasons: (i) total drug load scales with film surface area, allowing for a greater load per volume in a macroporous three dimensional substrate compared with a flat film; (ii) such a functionalized, combination osteoconductive/ osteoconductive scaffold is of interest by itself if biologic molecules can be applied to it in a way that increases bone formation for critical sized defects or when not enough autografted bone can be harvested; (iii) typically both an osteoinductive agent, such as BMP-2, and an osteoconductive microenvironment are necessary for ectopic bone formation. In the 3D-printed (3DP) β -tricalcium phosphate/polycaprolactone scaffolds used for this work, a precisely defined architecture can be employed, while taking advantage of the biocompatibility and bioactivity of the polymer material blend, allowing for a reasonable test substrate. It should be noted that these LbL coatings present a platform technology that can be applied to a very broad range of scaffold materials, devices or implant surfaces that have been optimized for specific applications.

Scaffold film coverage was probed using a fluorescent model protein, lysozyme (a model protein with similar isoelectric point and molecular weight to BMP-2) labeled with Alexa Fluor 488. Conformal surface coverage of the morphology of the 3DP scaffold (Figure 4) can be seen by visualizing the fluorescent LbL layer on top. 3D reconstruction assimilating all of the planes of focus shows a smooth coating in which the LbL film takes on the shape of the underlying popcorn-like scaffold surface.

[P2/chondroitin/BMP-2/chondroitin]₁₀₀ films constructed on the 3DP scaffolds show a distinct two-regime release profile (Figure 5). Very little burst release is seen from the film; compared with known clinical bulk collagen carriers and depots in which 40–60% of the encapsulated protein is immediately released in the first 3 hours with low therapeutic effect [26], here control over release leads to only 1% release in the same period, allowing the sustained release and interaction necessary to achieve bone development. A sustained linear release profile is observed for the first two days ($R^2 = 0.9848$) in which 80% of the film contents are released. The release profile then shifts to a second regime which is well fit to both linear ($R^2 = 0.96$) and power law ($R^2 = 0.997$) equations, in which the additional 20% of film release is sustained over an additional 2 weeks. A typical coated 3DP scaffold used

for *in vitro* and *in vivo* tests weighed 14 mg and released 10.6 \pm 0.3 μ g of total BMP-2 from the scaffold surface. The quantities released are on par with successful *in vivo* bulk release approaches, such as the collagen sponge, but the volumetric loading density of our LbL film (10 μ g BMP-2/mm³), is three orders of magnitude higher than typical bulk releasing films[24,25]. It is interesting to note that BMP-2 release can be controlled and sustained, even from such an ultrathin LbL coating.

To test for bioactivity of the coatings, MC3T3 E1 Subclone 4 pre-osteoblasts were exposed to (i) M - their normal growth medium (ii) D - growth medium plus β glycerol phosphate and L-ascorbic acid (differentiation medium) (iii) B - (D) with 90 ng/mL BMP-2 from stock, or (iv) R - (D) with 90 ng/mL BMP-2 released from an LbL film. Alkaline phosphatase (AP) serves as a standard early marker of induction of new bone differentiation from progenitor cells. In Figure 6, AP is markedly increased by BMP-2 LbL films compared with control films. Furthermore, cultures which have been induced to bone differentiation are able to form calcium deposition in the extracellular matrix (Alizarin Red staining) upon maturation, in addition to mineralization of the calcium deposits by incorporation of phosphate ions (Von Kossa staining). In Figure 6, staining of Alizarin Red and Von Kossa confirm osteoblast differentiation to a mature bone phenotype from BMP-2 exposure.

This result can also be quantified in the case of AP and Alizarin Red using spectrophotometric tests [16]. Interestingly, quantification for each data set (right hand panel) suggests that BMP-2 released from the LbL films shows *increased* gene induction and resulting differentiation within statistical significance (ANOVA analysis) compared to matched concentrations of BMP-2 supplemented directly to the medium. We hypothesize that the effective BMP-2 concentration perceived by the cells was increased due to the presence of Poly2 and chondroitin sulfate in the LbL release solution, possibly due to synergistic complexation of the biopolymer with sites on the BMP-2 protein and on the cell membrane surface. Thus, bioactivity of BMP-2 incorporated and released from LbL films remains intact.

We next turned to *in vivo* assays to probe whether the retained BMP-2 activity was robust enough to induce native host progenitor cells to initiate the bone differentiation cascade, creating bone in an intramuscular site. LbL coated scaffolds with or without incorporated BMP-2 were implanted in the rat quadriceps muscle (1 scaffold per animal). Micro computed tomography (MicroCT) images at four and nine week time points show large bone deposits created in response to BMP-2 LbL films. BMP-2 LbL implants (Figure 7, left) show new plate-like bone trabeculi that progressively increase in thickness from four to nine weeks. The bone forms with pattern fidelity to the underlying scaffold (central panels), underscoring the importance of the LbL slow-release carrier and BMP-2 surface concentration to bone formation, and new bone continued to be deposited even at 9 weeks. In contrast, no bone was formed in scaffolds coated with LbL films lacking BMP-2 (right panels). Thus BMP-2 released from LbL films can precipitate host progenitor cell induction to bone tissue. Quantification of the MicroCT images demonstrate an increase in bone mineral density (BMD) from four to nine weeks (right panel, Figure 7), consistent with continued maturation to more mineral dense bone.

Histological evaluation from the *in vivo* experiments further confirms ongoing, active deposition of mineralized bone matrix (Figure 8). Copious bone is found in full-thickness sections of BMP-2 releasing scaffolds at nine weeks; no bone was found in controls (Figure 8A & B). In LbL BMP-2 sections, cell types associated with healthy tissue remodelling dominate. The bone contains embedded osteocytes, osteoblasts lining the bone surface and laying down new bone, and cement lines from previous osteoblast expansions, consistent with active bone remodelling (Figure 8C). Hence, cell-free BMP-2 LbL implants are capable

of recruiting progenitor cells from the animal's native tissue and inducing a desired tissue response to implantation.

Bone maturation is also evident from histology. As bone matures, it goes from a woven, unorganized collagen matrix structure to a lamellar structure with aligned collagen fibrils that are birefringent under polarized light. The bone in Figure 8D and E has highly aligned collagen fibrils that indicate mature bone. Adipocytes are present in areas of mature lamellar bone, recapitulating the fatty marrow architecture and suggesting a high level of tissue maturation. Interestingly, not only are existing bone deposits maturing, but ongoing differentiation of host progenitor cells leads to new colonies of bone cells (Figure 8F). A cartilage intermediate is visible in the tissue induced by LbL BMP-2 films (Figure 8G,H) consistent with the anticipated endochondral bone formation process, in which cartilage is progressively replaced with bone. The recapitulation of bone architecture, cell phenotypes, placements, and the activation of further cell differentiation cascades, all precipitated by LbL released BMP-2 from the scaffold surface, show the tremendous impact that this technique can have on integration of implanted medical devices with surrounding tissue; none of the aforementioned biological processes is present in LbL scaffolds lacking BMP-2.

4. Conclusions

Localized release of biologics from implantable medical devices represents a powerful tool that can alter the course of healing and complications after implant deployment. As demonstrated here, micron-scale coatings of growth factors can wholly change the microenvironment to encourage bone tissue induction and in-growth to enhance integration with the implanted device. Here we demonstrate LbL coatings with high loading capacity that significantly exceeds typical biologic-encapsulating films, and capable of locally delivering the necessary microgram quantities of active growth factor to direct the native host cell response in a sustained manner as of yet unachievable with current depot devices.

Acknowledgments

This work was supported by the National Institutes of Health grant 1-R01-AG029601-01 and the Deshpande Center grant 009216-1. M.L.M. thanks the National Science Foundation for a graduate research fellowship. This work made use of MRSEC Shared Facilities supported by the National Science Foundation under Award Number DMR-0213282. The authors thank Jim Serdy and Thekken Spine, LLC for 3DP scaffold assistance.

References

1. Sheridan C. Fresh from the biologic pipeline-2009. *Nat Biotechnol* 2009;28(4):307–310. [PubMed: 20379168]
2. Lavernia CJ, Drakeford MK, Tsao AK, Gittelsohn A, Krackow KA, Hungerford DS. Revision and primary hip and knee arthroplasty - a cost-analysis. *Clin Orthop Relat Res* 1995;311:136–141. [PubMed: 7634568]
3. Fu K, Pack DW, Klibanov AM, Langer R. Visual evidence of acidic environment within degrading poly(lactic-co-glycolic acid) (PLGA) microspheres. *Pharm Res* 2000;17(1):100–106. [PubMed: 10714616]
4. Jewell CM, Lynn DM. Multilayered polyelectrolyte assemblies as platforms for the delivery of DNA and other nucleic acid-based therapeutics. *Adv Drug Deliv Rev* 2008;60(9):979–999. [PubMed: 18395291]
5. Schneider A, Vodouhe C, Richert L, Francius G, Le Guen E, Schaaf P, et al. Multifunctional polyelectrolyte multilayer films: Combining mechanical resistance, biodegradability, and bioactivity. *Biomacromolecules* 2007;8(1):139–145. [PubMed: 17206799]

6. Macdonald M, Rodriguez NM, Smith R, Hammond PT. Release of a model protein from biodegradable self assembled films for surface delivery applications. *J Control Release* 2008;131(3):228–234. [PubMed: 18721835]
7. Smith RC, Riollano M, Leung A, Hammond PT. Layer-by-Layer platform technology for small-molecule delivery. *Angew Chem Int Ed* 2009;48(47):8974–8977.
8. Shukla A, Fleming KE, Chuang HF, Chau TM, Loose CR, Stephanopoulos GN, et al. Controlling the release of peptide antimicrobial agents from surfaces. *Biomaterials* 31(8):2348–2357. [PubMed: 20004967]
9. Wood KC, Chuang Helen F, Batten Robert D, Lynn David M, Hammond Paula T. Controlling interlayer diffusion to achieve sustained, multiagent delivery from layer-by-layer thin films. *Proc Natl Acad Sci* 2006;103(27):10207–10212. [PubMed: 16801543]
10. Macdonald ML, Rodriguez NM, Shah NJ, Hammond PT. Characterization of tunable FGF-2 releasing polyelectrolyte multilayers. *Biomacromolecules* 2010;11(8):2053–2059. [PubMed: 20690713]
11. Crouzier T, Ren K, Nicolas C, Roy C, Picart C. Layer-By-Layer films as a biomimetic reservoir for rhBMP-2 delivery: Controlled differentiation of myoblasts to osteoblasts. *Small* 2009;5(5): 598–608. [PubMed: 19219837]
12. Facca S, Cortez C, Mendoza-Palomares C, Messadeq N, Dierich A, Johnston APR, et al. Active multilayered capsules for in vivo bone formation. *Proc Natl Acad Sci* 2010;107(8):3406–3411. [PubMed: 20160118]
13. Anderson DG, Lynn DM, Langer R. Semi-automated synthesis and screening of a large library of degradable cationic polymers for gene delivery. *Angew Chem Int Ed* 2003;42(27):3153–3158.
14. Lynn DM, Langer R. Degradable poly(beta-amino esters): synthesis, characterization, and self-assembly with plasmid DNA. *J Am Chem Soc* 2000;122(44):10761–10768.
15. Bragdon CR, Jasty M, Greene M, Rubash HE, Harris WH. Biologic fixation of total hip implants - Insights gained from a series of canine studies. *J Bone Joint Surg Am* 2004;86A:105–117. [PubMed: 15691115]
16. Gregory CA, Gunn WG, Peister A, Prockop DJ. An Alizarin red-based assay of mineralization by adherent cells in culture: comparison with cetylpyridinium chloride extraction. *Anal Biochem* 2004;329(1):77–84. [PubMed: 15136169]
17. Vazquez E, Dewitt DM, Hammond PT, Lynn DM. Construction of hydrolytically-degradable thin films via layer-by-layer deposition of degradable polyelectrolytes. *J Am Chem Soc* 2002;124(47): 13992–13993. [PubMed: 12440887]
18. Smith RC, Leung A, Kim BS, Hammond PT. Hydrophobic effects in the critical destabilization and release dynamics of degradable multilayer films. *Chem Mater* 2009;21(6):1108–1115. [PubMed: 20161308]
19. Jourdainne L, Arntz Y, Senger B, Debry C, Voegel JC, Schaaf P, et al. Multiple strata of exponentially growing polyelectrolyte multilayer films. *Macromolecules* 2007;40(2):316–321.
20. Lavallo P, Gergely C, Cuisinier FJG, Decher G, Schaaf P, Voegel JC, et al. Comparison of the structure of polyelectrolyte multilayer films exhibiting a linear and an exponential growth regime: An in situ atomic force microscopy study. *Macromolecules* 2002;35(11):4458–4465.
21. Porcel C, Lavallo P, Ball V, Decher G, Senger B, Voegel JC, et al. From exponential to linear growth in polyelectrolyte multilayers. *Langmuir* 2006;22(9):4376–4383. [PubMed: 16618190]
22. Porcel C, Lavallo P, Decher G, Senger B, Voegel JC, Schaaf P. Influence of the polyelectrolyte molecular weight on exponentially growing multilayer films in the linear regime. *Langmuir* 2007;23(4):1898–1904. [PubMed: 17279672]
23. Chuang HF, Smith RC, Hammond PT. Polyelectrolyte multilayers for tunable release of antibiotics. *Biomacromolecules* 2008;9(6):1660–1668. [PubMed: 18476743]
24. Degat MC, Dubreucq G, Meunier A, Dahri-Correia L, Sedel L, Petite H, et al. Enhancement of the biological activity of BMP-2 by synthetic dextran derivatives. *J Biomed Mater Res A* 2009;88A(1):174–183. [PubMed: 18286621]
25. Lin H, Zhaol Y, Sun WJ, Chen B, Zhang J, Zhao WX, et al. The effect of crosslinking heparin to demineralized bone matrix on mechanical strength and specific binding to human bone morphogenetic protein-2. *Biomaterials* 2008;29(9):1189–1197. [PubMed: 18083224]

26. Uludag H, Gao TJ, Porter TJ, Friess W, Wozney JM. Delivery systems for BMPs: Factors contributing to protein retention at an application site. *J Bone Joint Surg Am* 2001;83A:S128–S135. [PubMed: 11314790]

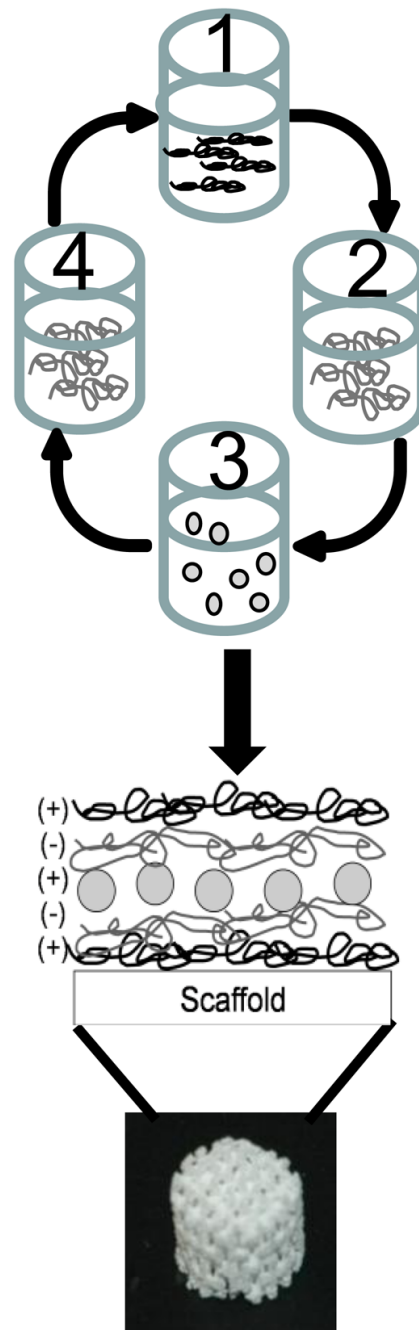


Figure 1.

Schematic of LbL architecture shows that a 3DP scaffold (or glass surface) is repeatedly dipped with tetralayer units consisting of (1) Poly 2 (positively charged), (2) chondroitin sulphate (negatively charged), (3) BMP-2 (positively charged) and (4) chondroitin sulfate. This tetralayer structure is repeated 100 times for all LbL films in this communication.

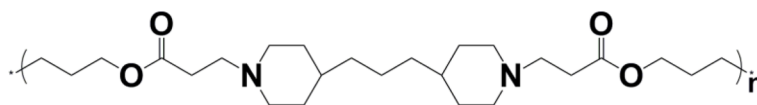


Figure 2.
Structure of Poly2, the selected poly(-aminoester) used in this work.

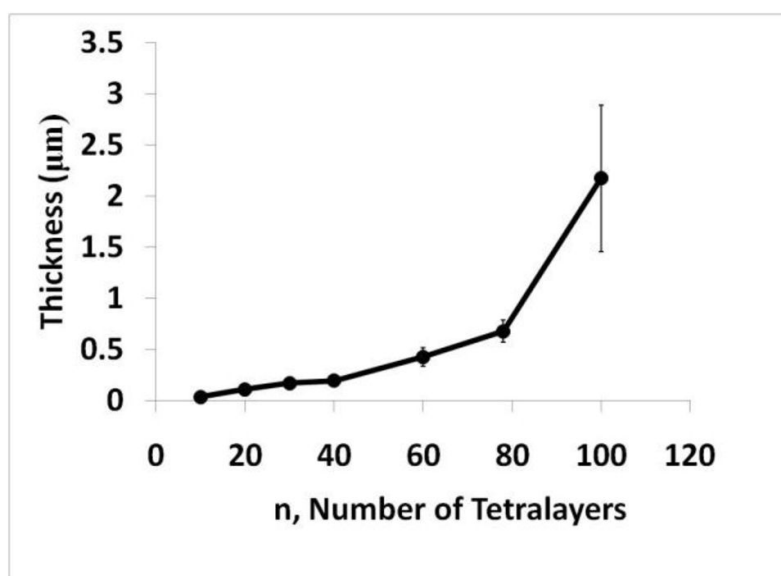


Figure 3. Profilometry measurements of LbL films built on glass allow for thickness analysis. Film thickness grows exponentially ($R^2 = 0.96$) with increasing numbers of tetralayers in a [P2/Chondroitin/BMP-2/Chondroitin] $_n$ film.

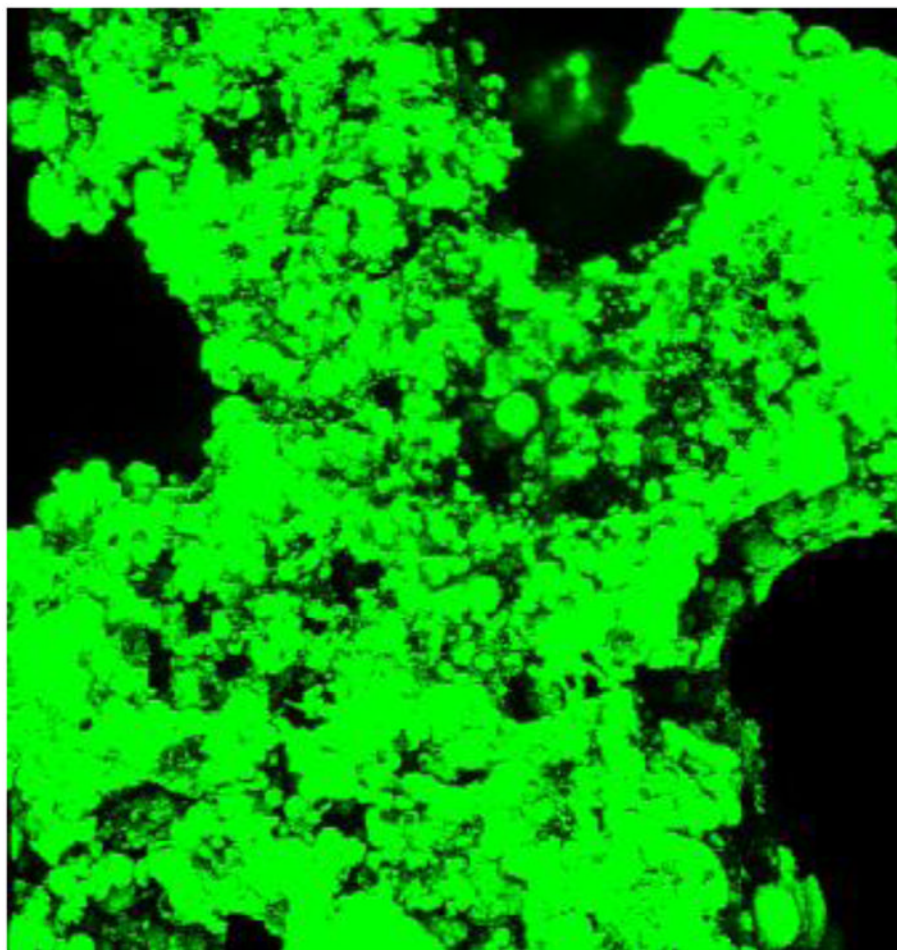


Figure 4. A 3DP β TCP-PCL blend scaffold was dipped with [P2/chondroitin/fluorescent lysozyme/chondroitin]₁₀₀. A three dimensional reconstruction of the resulting fluorescent LbL film shows a coating with conforms to the roughened, popcorn ball-like surface of the underlying 3DP scaffold.

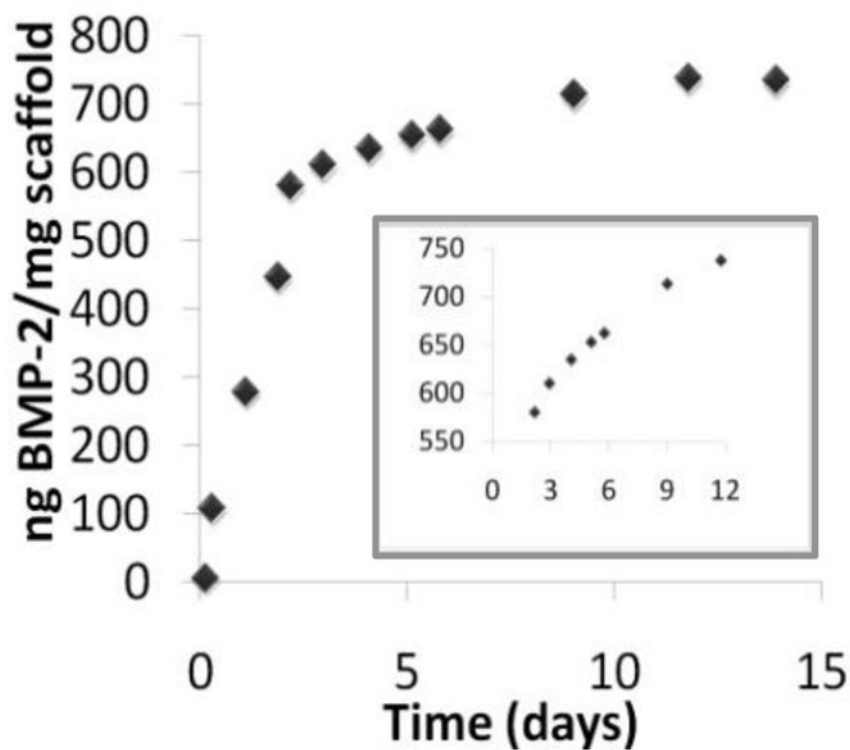


Figure 5. Release of BMP-2 from LbL films built on 3DP scaffold. Eighty percent of the material is released over a two day, linear release period. The remaining twenty percent is released over a period of approximately two weeks. Inset shows a blow up of the release profile after the initial two day period. Fourteen mg of scaffold were inserted in *in vivo* experiments; thus approximately 10 μ g of BMP-2 were released from scaffolds.

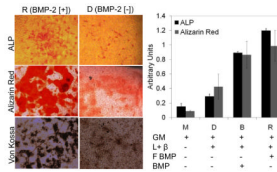


Figure 6.

Left panel: Bioactive BMP-2 released from LbL films (sample R) induces differentiation of MC3T3 pre-osteoblasts to an osteoblast phenotype compared with differentiation medium alone (sample D). Alkaline Phosphatase (ALP) staining (red) shows early (day 6) activation of the bone differentiation cascade; At 28 days of culture Alizarin Red staining for calcium deposition (red), and Von Kossa staining for mineralization of the calcium matrix (black) confirm the differentiation process to osteoblasts. Right panel: Quantification of the staining signal (3 readings on four independent experiments; error bar is standard deviation) shows that the increase in activity of BMP-2 released from LbL films (R) over BMP-2 positive control (B)(matched 90 ng/mL for both samples) is statistically significant. A single factor ANOVA test allowed rejection of the null hypothesis for both assays; a Tukey test showed that B and R are statistically different with $p < 0.01$ for ALP assay. Both B and R outperform differentiation medium alone (D) or growth medium alone (M). GM = growth medium; L+β = L-ascorbic acid and β-glycerol phosphate (differentiation factors); F BMP = LbL Film-released BMP-2; BMP = BMP-2 added directly to the medium.

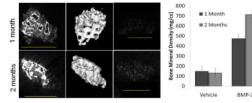


Figure 7.

Host progenitor cells exposed to LbL BMP-2 films undergo bone induction, creating calcium deposits visible with microCT in an intramuscular site. MicroCT 2-dimensional slices through the implant (top left panels) show that bone plate thickness is increasing with time; three-dimensional reconstructions (top middle panels) show remarkable pattern fidelity to the underlying scaffold, suggesting that bone grows in an outward-radiating pattern. Control films lacking BMP-2 show very little radio opacity (top right panels) indicating that BMP-2 is necessary for bone induction; three-dimensional images could not be reconstructed. In the bottom graph, bone mineral density, a marker of bone maturity, increases with implant age, indicating continual remodelling and maturing within the bone tissue. Scalebars are 4 mm.

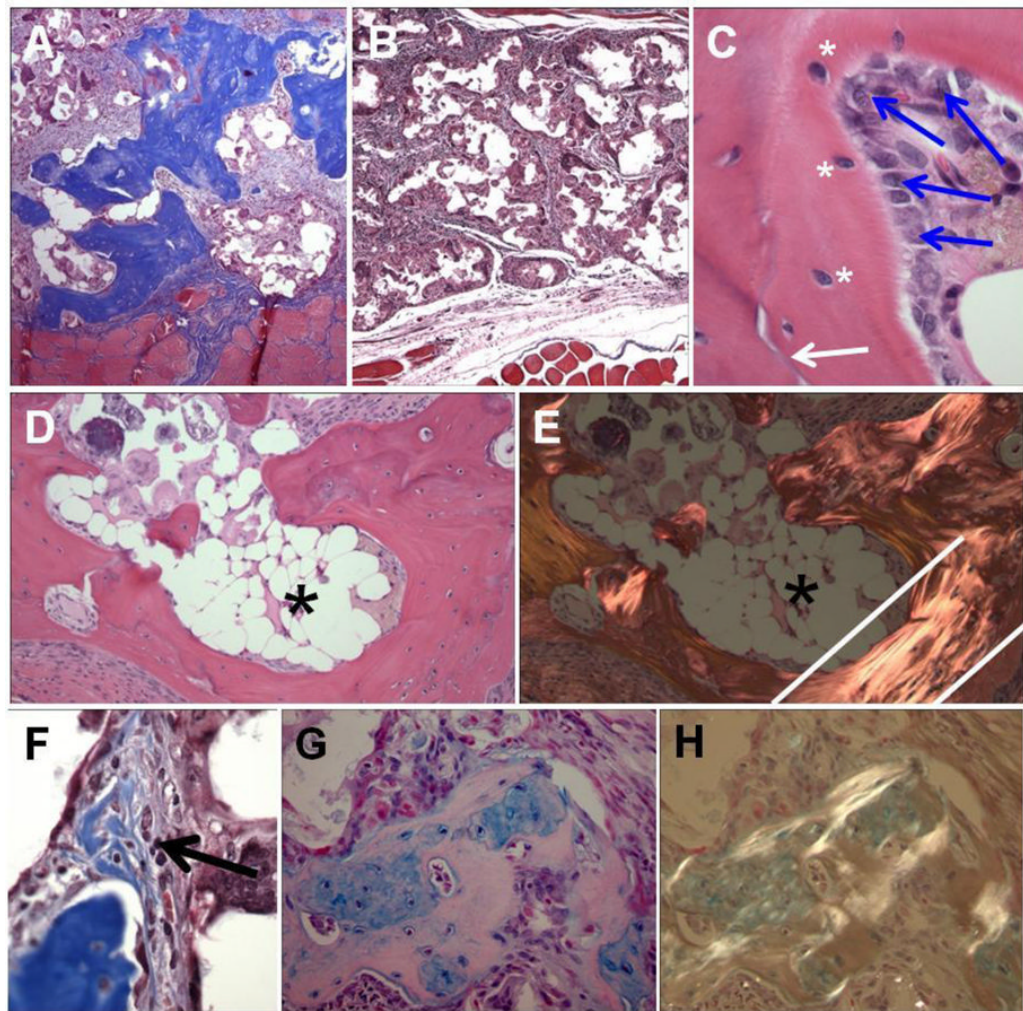


Figure 8.

Histologic findings from *in vivo* studies.. (A and B) Active scaffolds coated with BMP-2, Poly2, chondroitin sulfate film (A) and control scaffolds coated with Poly2 and chondroitin sulfate film (B), both at 9 weeks post-implantation. Brilliant blue staining of lamellar bone is seen in the active, but not control scaffolds (Masson trichrome stain, 40× original magnification). (C) Lamellar bone showing active bone formation with osteoblasts (blue arrows), mature osteocytes in lacunae (white asterisks) and cement line (white arrow) in active scaffolds at 9 weeks post-implantation. (H&E staining, 400× original magnification). (D and E) Mature lamellar bone with fatty marrow space (asterisk) under normal (D) and polarized light microscopy (E) at 9 weeks post-implantation. Note the bright signal from parallel collagen fibers indicating highly aligned lamellar bone, especially between the white lines. (H&E staining, 100× original magnification) (F) Woven bone formation (arrow) seen as a focus with pale blue staining and higher cellularity (black arrow) in contrast to the mature lamellar bone just below at 4 weeks post-implantation (Masson trichrome stain, 100× original magnification). (G and H) Cartilaginous intermediate areas (blue staining in G) are being remodeled into mature bone at 4 weeks post-implantation. The more mature areas brightly polarize while the immature cartilaginous areas do not (in H) (Alcian blue staining, 200× original magnification).